

# Effect of varied powder processing routes on the stabilizing performance and coordination type of polyacrylate in alumina suspensions

Conny Rödel<sup>a,\*</sup>, Martin Müller<sup>b</sup>, Maja Glorius<sup>b</sup>, Annegret Potthoff<sup>c</sup>, Alexander Michaelis<sup>a</sup>

<sup>a</sup> Institute of Material Science, Dresden University of Technology, 01062 Dresden, Germany

<sup>b</sup> Department of Polyelectrolytes and Dispersions, Leibniz Institute of Polymer Research e.V. (IPF), Hohe Strasse 6, 01069 Dresden, Germany

<sup>c</sup> Fraunhofer IKTS Dresden, Winterbergstrasse 28, 01277 Dresden, Germany

Received 6 May 2011; received in revised form 22 August 2011; accepted 29 August 2011

Available online 22 September 2011

## Abstract

The influence of initial pH and energy input during suspension homogenization on the stabilizing performance and coordination type of commercial available polyacrylate dispersant were studied. Additionally to widely used rheology and electroacoustic measurement techniques the alumina suspensions were analysed with centrifugal separation and in situ ATR-FTIR to study the impact of varied powder processing in detail. In contrast to zeta potential analysis and viscosity measurements only the determination of sedimentation properties by centrifugal separation shows the effect of macroscopic changes in powder processing. A combination of positively charged alumina surface and a high shear homogenization leads to the most stable suspension. Accordingly ATR-FTIR results show a correlation between improved suspension stability and inner-sphere coordination of polyacrylate. Moreover it was possible to determine an optimal pH range for inner-sphere adsorption. It can be shown that macroscopic changes in powder processing influence the coordination of dispersant and thus the suspension stability.

© 2011 Elsevier Ltd. All rights reserved.

**Keywords:** Processing; Suspension; Al<sub>2</sub>O<sub>3</sub>; Spectroscopy

## 1. Introduction

The knowledge about stabilization of dispersed phases plays an important role in many industrial applications such as pigments, paints, chemicals, cosmetics, drugs and ceramics. Especially for colloidal processing of ceramics in the micron and submicron range it is necessary to control the repulsive forces between the particles via addition of stabilizing agents to prevent agglomeration, lower the viscosity and reach an optimal homogenization of particles in the continuous phase. Therefore the control of chemical interactions at the ceramic/water interface is the fundamental step to zero-defect devices.<sup>1</sup> In general there are three main concepts to stabilize ceramic particles in polar media in order to overcome attractive interparticle forces: electrostatic, steric and electrosteric.<sup>2</sup> The electrostatic forces between particles are caused by excess electric charges, present

on and around the surface. Pure electrostatic stabilization of ceramic particles could be obtained via protonation by inorganic acids like nitric acid or by adsorption of low molecular weight organic acids, for instance by citric acid,<sup>3,4</sup> oxalic acid,<sup>5</sup> maleic acid<sup>6</sup> and benzene derivatives.<sup>7–10</sup> Steric stabilization presents an alternative way of controlling the colloidal stability. In this case repulsive forces are induced by an adsorbed layer of non-ionic organic molecules with a sufficient thickness to overcome the van der Waals attraction.<sup>11</sup> The combination of both mechanisms is called electrosteric stabilization. Commonly used dispersants for this concept are derived from polyacrylic acid and display a very efficient way to stabilize water based oxidic ceramic suspensions.<sup>12</sup>

Throughout the last decades there are numerous studies describing the interactions of carboxyl bearing organic molecules that are known to be very good dispersants for high concentrated alumina suspensions. Their impact is characterized by well-known rheology, electroacoustic and sedimentation measurement techniques. Depending on the molecular structure and number of functional groups the interactions of low

\* Corresponding author. Tel.: +49 351 2553 7650; fax: +49 351 2553 7610.  
E-mail address: [conny.roedel@tu-dresden.de](mailto:conny.roedel@tu-dresden.de) (C. Rödel).

molecular weight compounds is already described in detail by Hidber et al.<sup>7</sup>

Additionally in more recent work of e.g. Yoon the adsorption of low molecular weight compounds is analysed by means of in situ ATR-FTIR technique which was shown to be a powerful tool to analyse the specific chemical interactions between organic functionalities and Lewis acid centres like Al on the alumina.<sup>13,14</sup> These authors reported significant shifts for the systems oxalate/alumina,<sup>5</sup> citrate/alumina,<sup>6</sup> maleate/alumina<sup>14</sup> and other systems<sup>15–17</sup> in a series of papers. They did not assign these shifts to classical coordination types (unidentate, bridging etc.), which were reported even sooner by Deacon and Phillips<sup>18</sup> and McCluskey et al.<sup>19</sup> for carboxylates and metal ions. In fact Yoon et al. assigned the observed interactions to an “outer sphere” and an “inner sphere” coordination type, which are related to H-bonding or electrostatic in contrast to chemical ligand exchange interactions, respectively, between carboxylate groups and metal centres. Concerning our data on polyacrylate/alumina interaction in dependence of dispersion conditions we like to follow these lines for interpretation.

In contrast to low molecular weight compounds the interactions of polymeric dispersants within water based alumina suspensions are not fully investigated. Along with polyelectrolyte configuration<sup>20,21</sup> the stabilizing performance of polyelectrolyte dispersants were examined according to molecular weight<sup>22,23</sup> or with regard to chemical composition.<sup>24–26</sup> However, the influences of powder processing on the stability of polycarboxylate containing suspension and the interactions at the alumina/water interface have not been published so far.

In this study we present the results of an extensive suspension characterization by means of four different analysis methods including electroacoustic, rheological, centrifugal sedimentation and in situ ATR-FTIR measurements. The influence of energy input during homogenization and pH preadjustment on the stabilizing efficiency of a commercial available polyacrylate in aqueous alumina suspension is examined. It will be shown that an optimization in slip preparation can lead to a strengthened coordination of polyacrylate on the alumina surface which causes enhanced suspension stability.

## 2. Materials and methods

### 2.1. Powder and chemicals

A commercial alumina powder (Nabalox NO 625-10, Nabaltec, Germany) with a median particle size of 2.5  $\mu\text{m}$  (Mastersizer 2000, Malvern Instruments, England) was used as raw material. The powder exhibited a specific surface area of 2 m<sup>2</sup>/g (ASAP 2010, Micromeritics, USA) and a density of 3.98 g/cm<sup>3</sup> (Pentapycnometer, Quantachrome Instr., USA). The used dispersant was sodium polyacrylate (NaPA, 8000 g/mol, Sigma–Aldrich, Germany). Unless otherwise indicated, the concentration of the dispersant is given in weight percent (wt%) with respect to the solid content.

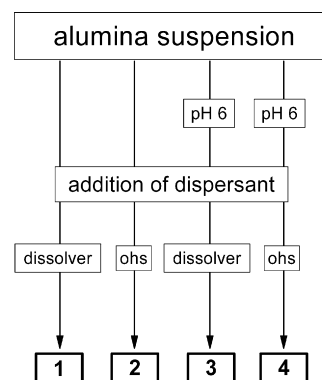


Fig. 1. Suspension preparation procedures. Starting with the bare suspension, samples 1 and 2 differ in the type of homogenization technique (ohs = overhead shaker) after addition of dispersant. Additionally the pH of samples 3 and 4 were preadjusted to a value of 6.

### 2.2. Sample preparation

Aqueous suspensions (60 wt%) were prepared by addition of alumina powder to deionized water under constant stirring using a laboratory dissolver stirrer (Ultra Turrax T50, IKA, Germany).

In the first part bare suspensions were spiked with different amounts of sodium polyacrylate up to 1 wt% relative to the content of solid alumina. The following homogenizations were performed on the one hand with the laboratory dissolver stirrer presenting a high shear mixing route and on the other hand with an overhead shaker (Heidolph Instruments, Germany) presenting a low shear mixing route (Fig. 1). In the second part the pH of bare suspensions were adjusted at a value of 6 with hydrochloric acid. Further addition of sodium polyacrylate and homogenization were executed as described above. With the mentioned preparation routine four types of samples were created and the influence of energy input during homogenization and/or pH adjustment on the stabilizing performance of sodium polyacrylate was investigated.

According to Meyer et al. changes in polymer properties during homogenization were not expected. Hence the absolute energy input during a 10 minute homogenization using a laboratory dissolver stirrer is too low to alter the molecular mass or architecture.<sup>27</sup>

### 2.3. Electroacoustic measurements

To study changes in powder surface charge by addition of dispersing agent or acid, ESA measurements were performed as described in the literature<sup>28</sup> using the Zetaprobe measurement system (Colloidal Dynamics, USA). Measurement conditions retained constant 25 °C by application of an external thermosta-tization and continuous stirring of the sample.

### 2.4. Rheological measurements

Changes in viscosity due to dosage of additive or the procedure of suspension preparation were determined using the rotational and oscillating viscometer MCR 101 (Anton Paar GmbH, Austria). The flow characteristics were analysed at 25 °C

using rotational measurements with a double gap measuring system at several shear rates from  $10 \text{ s}^{-1}$  up to  $1000 \text{ s}^{-1}$ . Before starting measurement, pre-shearing was performed in order to transmit the same rheological history to all the samples being tested. For comparison, the viscosity values at a shear rate of  $100 \text{ s}^{-1}$  were used.

### 2.5. Centrifugal sedimentation

The analytical centrifuge LUMiSizer (LUM GmbH, Germany) was used to study the sedimentation properties in a centrifugal field. Shape and progression of sedimentation profiles contain information about the kinetics of separation process and allows the evaluation of particle–particle interactions.<sup>29–32</sup> In this case sedimentation experiments were carried out to determine the settling velocity of particles and the sedimentation height as a function of dispersant amount and type of sample preparation. All measurements were executed at  $25^\circ\text{C}$  and a relative centrifugal force of 110 g.

### 2.6. ATR-FTIR measurements

Attenuated total reflection (ATR) Fourier transform infrared (FTIR) spectroscopy was used to obtain information on the interaction type between carboxyl based dispersing agents and the alumina surface. All ATR-FTIR measurements were performed on a FTIR spectrometer (Vertex 70, Bruker Optics GmbH, Germany) equipped with globar source and a ditriglycinesulfate (DTGS) detector. The ATR-attachment consisted of a commercial four-mirror-attachment (Wilks Enterprise Inc., East Norwalk, USA) and homebuilt flow-through cell (U.P. Fringeli, Zurich) housing a trapezoidal ZnSe internal reflection element (IRE) with dimensions  $50 \text{ mm} \times 20 \text{ mm} \times 2 \text{ mm}$ . The angle of incidence was  $45^\circ$  resulting in 11 active reflections on one side of the IRE. ATR-FTIR spectra were recorded in the single beam mode. That means, ATR-FTIR absorbance spectra of the suspensions were obtained from the ratio of the single channel spectrum of ZnSe in contact to the suspension ( $I$ ) and the single channel spectrum of pure water or of the respective solvent of the suspension ( $I_0$ ) according to  $A = -\log I/I_0$ . All measurements were performed at  $22^\circ\text{C} \pm 0.5 \text{ K}$ . To prevent sedimentation, the suspensions were circulated at a velocity of  $0.5 \text{ mL/min}$ .

The application of ATR-FTIR using ZnSe IRE instead of transmission FTIR using e.g.  $\text{CaF}_2$  cuvettes is justified by the fact, that in ATR-FTIR mode even for 11 reflections an effective thickness (“pathlength”) introduced by Harrick<sup>33</sup> of smaller than  $5 \mu\text{m}$  in comparison to transmission cuvettes, which cannot be routinely constructed with pathlengths lower than  $10\text{--}20 \mu\text{m}$ . Too large pathlengths have the disadvantage of insufficient compensation of the intense water absorptions at  $3400 \text{ (}\nu(\text{OH})\text{)}$  and  $1640 \text{ cm}^{-1}$  ( $\delta(\text{OH})$ ). However, the pathlength should also be not too small since the IR bands of NaPA must be sufficiently intense. Fortunately, in this study identical suspension samples with NaPA concentrations of  $0.03 \text{ M}$  could be used for the electroacoustic, rheological, centrifugal sedimentation and ATR-FTIR measurements. Furthermore, it was checked, if NaPA formed an adsorbed surface layer onto the ZnSe IRE, which was

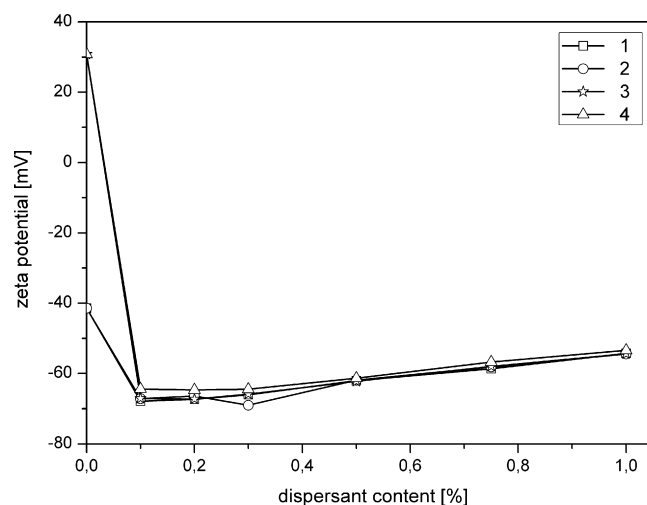


Fig. 2. Zeta potential of alumina particles as a function of relative dispersant content with regard to various suspension preparation procedures (1–4).

addressed by comparing related ATR-FTIR spectra before and after rinsing with pure water. Since in our samples NaPA was always completely rinsed off, the ATR-FTIR spectra reflected NaPA interacting with alumina and not with ZnSe.

The measured ATR-FTIR spectra were baseline corrected between  $1800$  and  $1300 \text{ cm}^{-1}$  with the OPUS 5.0 program (Bruker Optics GmbH, Germany) using three fixed points. For a quantitative peak analysis curve fitting with 50% Lorentzian and 50% Gaussian line shape was applied to the baseline corrected ATR-FTIR spectra (OPUS 5.0, Bruker Optics GmbH, Germany). A detailed description will be published elsewhere. Generally, a concept of line shape analysis was followed similar to one, which was reported earlier therein<sup>34</sup> and used for quantitative peptide conformation analysis. Briefly, all spectra in the range from  $1800$  to  $1300 \text{ cm}^{-1}$  shown in this study were fitted by the superposition of 7 components (50% Lorentz/50% Gauss). In a first run all spectra were fitted (least squares) under relaxation of the three parameters position, half width and intensity for every of the 7 components. The obtained parameters for half width and position were averaged for every component (1–7) and with these averaged parameter values a final constraint fit under fixation of half width and position and free relaxation of the intensities was performed for every spectrum. A convenient representation of the original line shape could be achieved (data not shown herein). The ratio of the components 3 ( $1405 \text{ cm}^{-1}$ ) and 4 ( $1360 \text{ cm}^{-1}$ ) were plotted versus pH value below in Fig. 8.

## 3. Results and discussion

### 3.1. Electroacoustic measurements

In Fig. 2 the zeta potential is plotted versus the amount of added sodium polyacrylate in wt% with respect to content of solid alumina. It can be seen that the addition of dispersant has a significant effect on the surface charge properties in all cases which possess an attractive interaction between polyacrylate molecules and the alumina surface. Even  $0.1\text{--}0.2 \text{ wt}\%$  dispersant are enough to generate a strong negative surface potential,

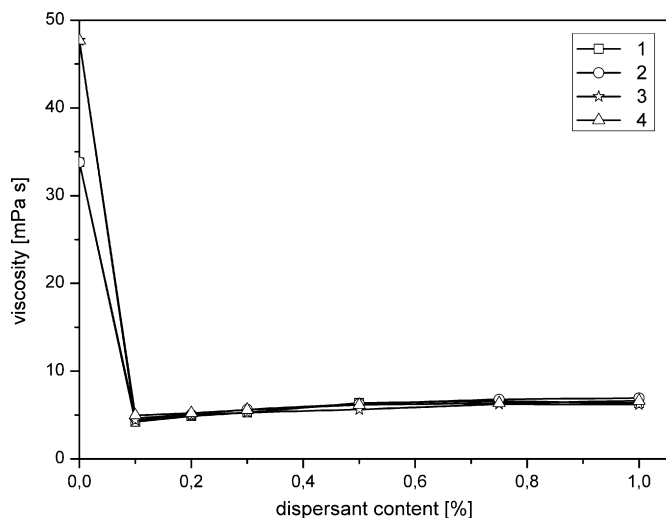


Fig. 3. Viscosity of alumina suspensions as a function of relative dispersant content with regard to various suspension preparation procedures (1–4).

which indicates a good suspension stability. Further polymer addition causes an increase of zeta potential due to rising ionic strength of aqueous media and thus a compression of the electric double layer occurs leading to a slightly destabilization of suspension. So 0.2 wt% sodium polyacrylate marks the optimum dispersant amount for the analysed suspension.

However, there are no indications for different types of interactions between polyacrylate and alumina surface depending on the sign of surface potential which can be presetted with the pH value of suspension or energy input during homogenization. In terms of electroacoustic measurement technique the negatively charged polyacrylate adsorbs on negatively charged alumina surface with an initial surface potential of  $-40$  mV (samples 1 and 2) as well as on positive charged ones with an initial surface potential of  $30$  mV (samples 3 and 4). Hence the differences of varied sample preparations by energy input and/or pH preadjustment cannot be detected in detail with this characterization method.

### 3.2. Rheological measurements

The rheological behaviour of the suspensions expressed by viscosity curves as a function of polyacrylate content is shown in Fig. 3. Starting points in the case of dispersant free suspensions were  $34$  mPa s (samples 1 and 2) and  $48$  mPa s (samples 3 and 4) caused by the different pH values of the suspensions. All samples possess an obvious decrease in viscosity after the addition of small amounts of dispersant and exhibit a shear thinning behaviour. Accordingly sodium polyacrylate is applicable to lower the viscosity of alumina suspensions through enhancement of interparticle repulsive forces. The results of rheological characterizations are consistent with the mentioned electrophoretic effects. It can be seen that the lowest viscosities are reached at dispersant amounts of  $0.1$  wt%. Further polyacrylate addition does not lead to further improvement of rheological properties. However, significant differences between the samples are not obvious.

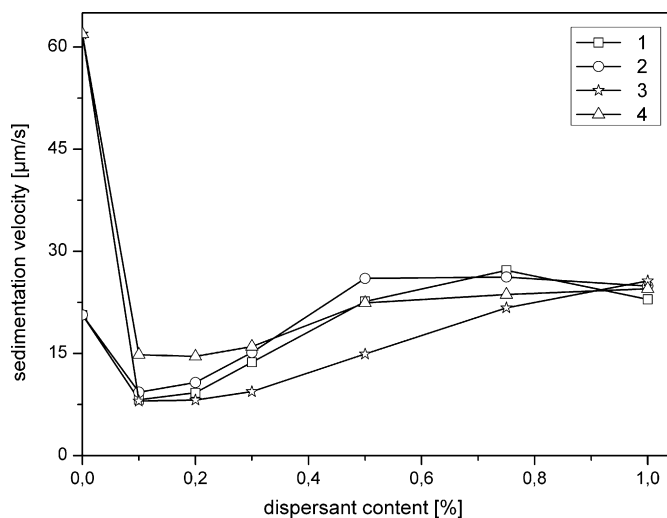


Fig. 4. Sedimentation velocity of alumina particles as a function of relative dispersant content with regard to various suspension preparation procedures (1–4).

### 3.3. Centrifugal sedimentation

The results of the sedimentation measurements are presented in Figs. 4 and 5. Comparable to the findings above the settling velocities of particles show a significant decrease after the addition of sodium polyacrylate indicating its stabilizing effect. Also the local minimum introducing the optimum dispersant amount occurs. Obviously, it is possible to get more information about the state of suspension from the presented curves. The differences between the samples can be correlated to varied preparation routes. Samples 1 and 2 are showing a rather similar progression, where the high shear homogenization provides slightly lower settling velocities in the range of optimum dispersant amount around  $0.2$  wt%. In the case of pH preadjusted samples 3 and 4 this difference is getting even

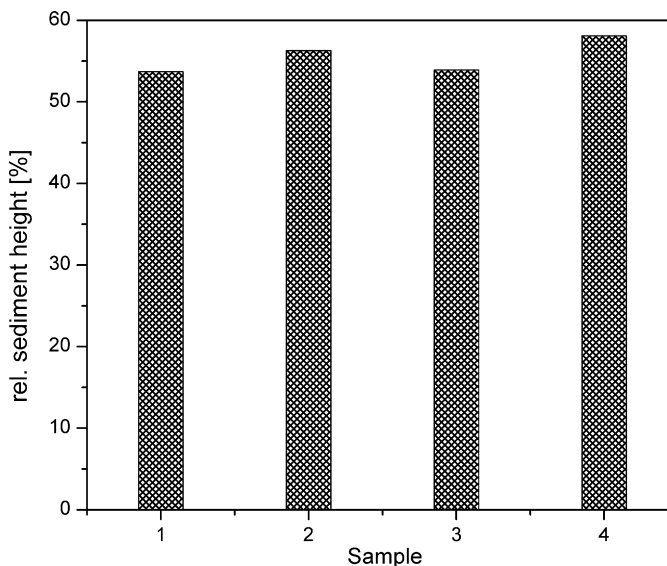


Fig. 5. Relative sediment heights of alumina suspensions ( $0.2$  wt% NaPA) according to various suspension preparation procedures (1–4).



more distinct. Obviously the homogenization under high shear conditions has a positive effect on the stabilizing performance of polyacrylate dispersant. The comparison of samples 1 and 3 shows that the combination of pH preadjustment and high shear homogenization leads to the lowest settling velocities at all.

Changes in sedimentation behaviour due to differences in state of particle agglomeration are not expected. Because alterations in agglomeration state is on the one hand governed by interparticle forces and on the other hand can be monitored with both sedimentation as well as viscosity measurement techniques. In our case the highly negative zeta potential of about  $-70$  mV induced by polyacrylate dispersant ensure strong repulsive interparticle forces within the entire concentration range. Thus a stable suspension of fully deagglomerated particles is assumed. Additionally viscosity measurements are sensitive for changes in state of particle agglomeration, but there are no changes noticeable independent from the way of sample preparation. Anyway, different agglomeration states induce both altered sedimentation behaviour and changed suspension viscosity. In the presented results only changes in sedimentation behaviour were determined. Hence the state of agglomeration was expected to be comparable.

Furthermore the sediment heights of samples with 0.2 wt% polyacrylate were measured and compared to each other. In Fig. 5 the relative sediment heights are shown in relation to absolute filling level in the cuvette. According to the literature low density sediments with a larger volume relate to unstable suspensions, whereas high density sediments with a lower volume indicate a good stabilization of primary particles.<sup>35–37</sup> It can be noticed that the sedimentation heights of high shear treated samples show a minimum of the settled volume, which cannot be correlated with the determined zeta potential values reported in Fig. 2. Hence, to clarify the differences in settling velocity and sediment height it is necessary to study the chemical interactions at the alumina/water interface in detail.

### 3.4. ATR-FTIR measurements

To study chemical interactions such as surface coordination of polyacrylate to alumina in more detail in situ ATR-FTIR measurements were performed. For that suspensions containing 60 wt% alumina and 0.2 wt% sodium polyacrylate related to the alumina content, which is equivalent to a NaPA concentration of 0.03 M, were used. These samples were different from the energy input during homogenization and the preadjustment of the pH and were equivalent to those measured by the electroacoustic, rheological and settlement measurements.

The measured and baseline corrected ATR-FTIR spectra of these four suspensions are illustrated in Fig. 6. The spectra of the samples prepared without pH preadjustment (1 and 2) are dominated by the  $\nu_a(\text{COO}^-)$  and  $\nu_s(\text{COO}^-)$  bands at 1555 and 1405  $\text{cm}^{-1}$ , respectively, of the carboxyl groups of polyacrylate. However, a shoulder at the lower wavenumber of 1360  $\text{cm}^{-1}$  can be rationalized as a downshift of the  $\nu_s(\text{COO}^-)$  band indicating an “inner-sphere” coordination of carboxyl groups of polyacrylate to the alumina surface. Similar shifts of polyacrylates at alumina, kaolin, hematite, and  $\text{TiO}_2$  systems have been reported

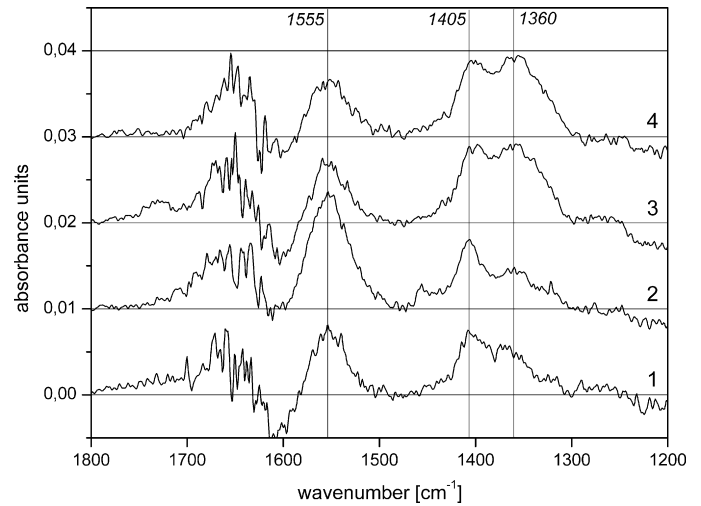


Fig. 6. ATR-FTIR spectra of alumina suspensions (0.2 wt% NaPA) made by the four different preparation routines (1–4). Indicated values are in  $\text{cm}^{-1}$ .

by Vermöhlen et al.,<sup>38</sup> Taylor and Sigmund,<sup>39</sup> Zaman et al.,<sup>40</sup> Kirwan et al.,<sup>41</sup> Li and Tripp,<sup>42</sup> Montavon et al.,<sup>43</sup> Lee et al.<sup>44,45</sup> and Jones et al.<sup>46</sup>

Only slight differences can be observed between the samples 1 and 2 and between 3 and 4. In case of homogenization with the dissolver (high energy input) the shoulder at 1360  $\text{cm}^{-1}$  is more distinctive than in case of homogenization with the overhead shaker (low energy input). So, it can be reasoned that high energy input results in a better coordination of polyacrylate to the alumina surface. The spectra of the suspensions homogenized with pH adjustment to pH 6 before sodium polyacrylate addition (3, 4) demonstrate a strong and separated peak at 1360  $\text{cm}^{-1}$  additional to the  $\nu_a(\text{COO}^-)$  and  $\nu_s(\text{COO}^-)$  band at 1555 and 1405  $\text{cm}^{-1}$ , which indicates “inner-sphere” coordination between the polyacrylate and the alumina surface. Obviously, the adjustment of the pH value from 10 (original pH of the alumina suspension) to 6 leads to a positive charge of the alumina surface and therefore to a more effective coordination between polyacrylate and alumina. From these results it can be reasoned that the pH of the suspension has an important influence on the coordination strength of the polyacrylate to the alumina surface and thus to macroscopic stability.

To study the pH influence in more detail, a suspension containing 60 wt% alumina and 0.2 wt% sodium polyacrylate was subsequently titrated with 1 M hydrochloric acid from pH 10 to pH 1.7 and probed by ATR-FTIR spectroscopy. Fig. 7 shows the related measured and baseline corrected ATR-FTIR spectra in the 1800–1250  $\text{cm}^{-1}$  region. Analogously to the spectra in Fig. 6 in the initial spectrum at pH 10 beside the two diagnostic peaks at 1555 and 1405  $\text{cm}^{-1}$  of the  $\nu_a(\text{COO}^-)$  and  $\nu_s(\text{COO}^-)$  bands again a shoulder at 1360  $\text{cm}^{-1}$  can be observed indicating inner sphere coordination. Decreasing the pH down to pH 7.8 the shoulder at 1360  $\text{cm}^{-1}$  further increases forming finally a separated peak, whereas the peak at 1405  $\text{cm}^{-1}$  decreases. Interestingly, in the spectrum at pH 7.8 these two peaks have comparable absorbance. The  $\nu_a(\text{COO}^-)$  band at 1555  $\text{cm}^{-1}$  shows no shift over the whole pH range.

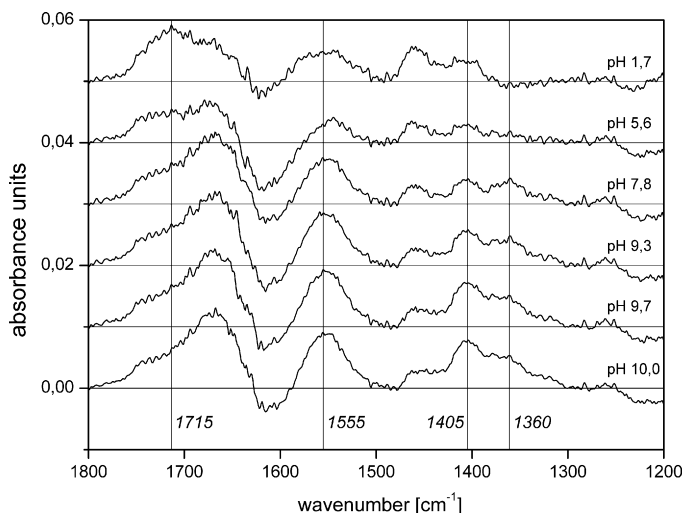


Fig. 7. ATR-FTIR spectra of alumina suspension (0.2 wt% NaPA) titrated with 1 M hydrochloric acid from pH 10 to pH 1.7. Indicated values are in  $\text{cm}^{-1}$ .

To get quantitative information on the intensities of the peaks at  $1405 \text{ cm}^{-1}$  and  $1360 \text{ cm}^{-1}$  as well as their ratio curve fitting analysis based on totally 7 individual band components was applied to the spectra shown in Fig. 7 (see Section 2). In Fig. 8 the ratio of the components at  $1405$  and  $1360 \text{ cm}^{-1}$  are plotted versus the pH value. At first between pH 10 down to pH 7.8 the  $1360/1405$  ratio increases from around 0.6 up to a maximum of 1. Further lowering the pH the  $1360/1405$  ratio falls off again until the vibration band at  $1360 \text{ cm}^{-1}$  disappears at pH values below 5.6 and the ratio gets zero. Additionally, at these acidic pH values a band at  $1717 \text{ cm}^{-1}$  appears, which can be assigned to the  $\nu(\text{C}=\text{O})$  of carboxylic acid groups in polyacrylate.

The following scenario seems to be evident in polyacrylate/alumina suspensions with varying pH values: Starting at pH = 10 polyacrylate bears carboxylate groups and high negative charge density. Alumina has also negative net charge leading to polyacrylate/alumina repulsion and thus to outer sphere

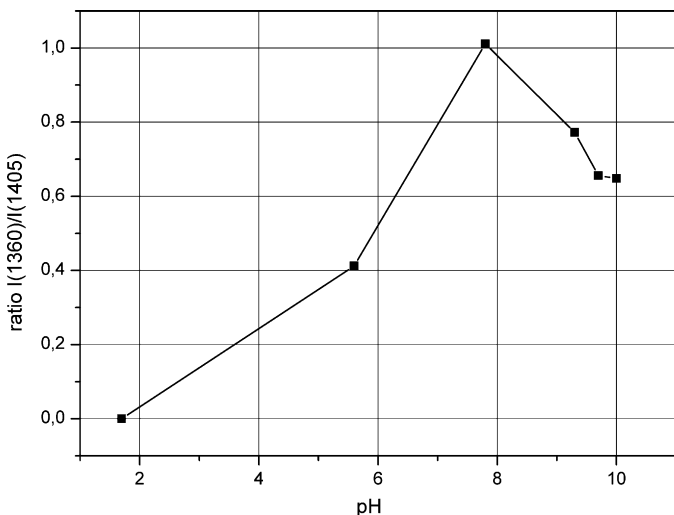


Fig. 8. Ratio of the symmetric vibration band at  $1405 \text{ cm}^{-1}$  and the “inner-sphere” band at  $1360 \text{ cm}^{-1}$  as a function of pH.

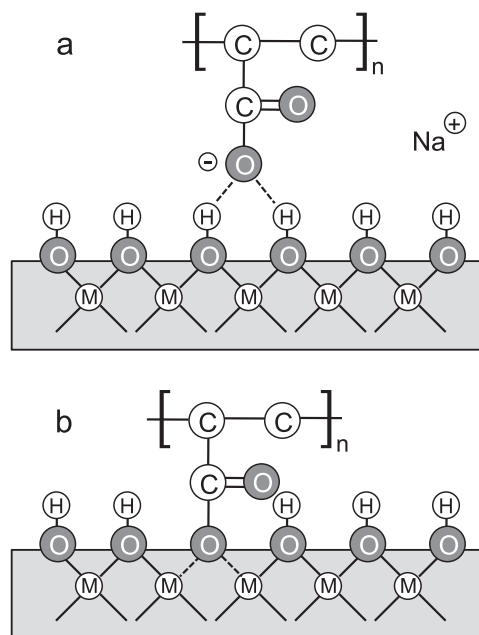


Fig. 9. Schematic drawings of outer sphere adsorbed polyacrylate (a) and inner sphere adsorbed polyacrylate (b) at the alumina/water interface in imitation on Yoon et al.<sup>15</sup> (hydrogen atoms at the polyacrylate backbone are not shown).

adsorption (Fig. 9a). Decreasing subsequently the pH to 7.8 polyacrylate remains negatively charged but alumina adopts a slight positive net charge resulting in polyacrylate/alumina attraction, which might favour the inner sphere coordination (Fig. 9b). At the  $\text{pH} < 5.6$  polyacrylate is partly protonated and neutral, while alumina has a marked positive net charge leading to no significant polyacrylate/alumina attraction and again a loss of inner sphere character. Hence, most importantly Fig. 8 demonstrates that pH values in the quasineutral cause a maximum in coordination strength between polyacrylate and alumina.

#### 4. Conclusions

On the basis of electroacoustic, rheological and centrifugal sedimentation measurements, it could be shown, that the stabilizing performance of polyacrylate on highly concentrated alumina suspensions could be significantly improved due to the increase of energy input during suspension homogenization and/or pH preadjustment.

By means of centrifugal separation analysis it was possible to visualize the effect of macroscopic changes in powder processing on type of polyacrylate coordination in molecular level. The determination of sedimentation properties especially settling velocity and sediment height via centrifugal separation analysis displays a simple and very effective way to get information about interparticle forces within slightly different suspensions. It has been found that this characterization method exhibits a useful extension to the widely used rheology and electroacoustic measurement techniques.

These significant macroscopic effects were addressed by in situ ATR-FTIR spectroscopy, which was shown to be a powerful tool to measure alumina/polyacrylate suspension samples

identical to those measured by the above mentioned techniques in order to elucidate molecular interactions. Based on a downshift of the symmetric carboxylate stretching band from 1405 to 1360  $\text{cm}^{-1}$  a differentiation between inner and outer sphere coordination could be performed. Thereby the 1360  $\text{cm}^{-1}$  component could be molecularly assigned to an inner sphere coordination state of polyacrylate and could be macroscopically correlated to the suspension stability performance. Plotting the 1360/1405 ratio versus the pH value it was possible to identify a pH between 7 and 8 as optimum for inner sphere coordination.

Generally it could be demonstrated that the achievement of a better understanding about chemical interactions of macromolecular polyelectrolytes at the ceramic/water interface is closely connected with the correlation of multiple complementary characterization methods.

## References

- Lange FF. Powder processing science and technology for increased reliability. *J Am Ceram Soc* 1989;**72**:3–15.
- Lewis JA. Colloidal processing of ceramics. *J Am Ceram Soc* 2000;**83**:2341–59.
- Hidber PC, Graule TJ, Gauckler LJ. Citric acid – a dispersant for aqueous alumina suspensions. *J Am Ceram Soc* 1996;**79**:1857–67.
- Liu YQ, Gao L, Guo J. Comparative study on the stabilizing effect of 2-phosphonobutane-1,2,4-tricarboxylic acid and citric acid for alumina suspensions. *Colloids Surf A* 2001;**193**:187–95.
- Johnson SB, Yoon TH, Slowey AJ, Brown GE. Adsorption of organic matter at mineral/water interfaces: 3. Implications of surface dissolution for adsorption of oxalate. *Langmuir* 2004;**20**:11480–92.
- Johnson SB, Brown GE, Healy TW, Scales PJ. Adsorption of organic matter at mineral/water interfaces: 6. Effect of inner-sphere versus outer-sphere adsorption on colloidal stability. *Langmuir* 2005;**21**:6356–65.
- Hidber PC, Graule TJ, Gauckler LJ. Influence of the dispersant structure on properties of electrostatically stabilized aqueous alumina suspensions. *J Eur Ceram Soc* 1997;**17**:239–49.
- Laucournet R, Pagnoux C, Chartier T, Baumard JF. Catechol derivatives and anion adsorption onto alumina surfaces in aqueous media: influence on the electrokinetic properties. *J Eur Ceram Soc* 2001;**21**:869–78.
- Studart AR, Pandolfelli VC, Tervoort E, Gauckler LJ. Selection of dispersants for high-alumina zero-cement refractory castables. *J Eur Ceram Soc* 2003;**23**:997–1004.
- Jiang LQ, Gao L, Liu YQ. Adsorption of salicylic acid, 5-sulfosalicylic acid and Tiron at the alumina–water interface. *Colloids Surf A* 2002;**211**:165–72.
- Hazan Y, Reuter T, Werner D, Clasen R, Graule T. Interactions and dispersion stability of aluminium oxide colloidal particles in electroless nickel solutions in the presence of comb polyelectrolytes. *J Colloid Interface Sci* 2008;**323**:293–300.
- Cesarano III J, Aksay IA. Processing of highly concentrated aqueous  $\alpha$ -alumina suspensions stabilized with polyelectrolytes. *J Am Ceram Soc* 1988;**71**:1062–7.
- Yoon TH, Johnson SB, Musgrave CB, Brown GE. Adsorption of organic matter at mineral/water interfaces: I. ATR-FTIR spectroscopic and quantum chemical study of oxalate adsorbed at boehmit/water and corundum/water interfaces. *Geochim Cosmochim Acta* 2004;**68**:4505–18.
- Johnson SB, Yoon TH, Kocar BD, Brown GE. Adsorption of organic matter at mineral/water interfaces: 2. Outer-sphere adsorption of maleate and implications for dissolution process. *Langmuir* 2004;**20**:4996–5006.
- Yoon TH, Johnson SB, Brown GE. Adsorption of organic matter at mineral/water interfaces: IV. Adsorption of humic substances at boehmit/water interfaces and impact on boehmite dissolution. *Langmuir* 2005;**21**:5002–12.
- Johnson SB, Yoon TH, Brown GE. Adsorption of organic matter at mineral/water interfaces: 5. Effects of adsorbed natural organic matter analogues on mineral dissolution. *Langmuir* 2005;**21**:2811–21.
- Ha J, Yoon TH, Wang Y, Musgrave CB, Brown GE. Adsorption of organic matter at mineral/water interfaces: 7. ATR-FTIR and quantum chemical study of lactate interactions with hematite nanoparticles. *Langmuir* 2008;**24**:6683–92.
- Deacon GB, Phillips RJ. Relationships between the carbon–oxygen stretching frequencies of carboxylate complexes and the type of carboxylate coordination. *Coord Chem Rev* 1980;**33**:227–50.
- McCluskey PH, Snyder RL, Condrate RA. Infrared spectral studies of various metal polyacrylates. *J Solid State Chem* 1989;**83**:332–9.
- Chibowski S, Opala Mazur E, Patkowski J. Influence of the ionic strength on the adsorption properties of the system dispersed aluminium oxide–polyacrylic acid. *Mater Chem Phys* 2005;**93**:262–71.
- Lyklema J, Fleer GJ. Electrical contributions to the effect of macromolecules on colloid stability. *Colloids Surf* 1978;**25**:357–68.
- Santhiya D, Nandini G, Subramanian S, Natarajan KA, Malghan SG. Effect of polymer molecular weight on the adsorption of polyacrylic acid at the alumina–water interface. *Colloids Surf A* 1998;**133**:157–63.
- Das KK, Somasundaran P. Flocculation–dispersion characteristics of alumina using a wide molecular weight range of polyacrylic acids. *Colloids Surf A* 2003;**223**:17–25.
- Baklouti S, Romdhane MRB, Boufi S, Pagnoux C, Chartier T, Baumard JF. Effect of copolymer dispersant structure on the properties of alumina suspensions. *J Eur Ceram Soc* 2003;**23**:905–11.
- Bouhamed H, Boufi S, Magnin A. Alumina interaction with AMPS-PEG random copolymer. II. Stability and rheological behavior. *Colloids Surf A* 2005;**253**:145–53.
- Kamiya H, Fukuda Y, Suzuki Y, Tsukada M, Kakui T, Naito M. Effect of polymer dispersant structure on electrosteric interaction and dense alumina suspension behavior. *J Am Ceram Soc* 1999;**82**:3407–12.
- Meyer A, Lenzner K, Potthoff A. Influence of energy input on suspension properties. *Adv Sci Technol* 2010;**62**:141–6.
- Greenwood R. Review of the measurement of zeta potentials in concentrated aqueous suspensions using electroacoustics. *Adv Colloid Interface Sci* 2003;**106**:55–81.
- Sobisch T, Lerche D. Application of a new separation analyzer for the characterisation of dispersions stabilized with clay derivatives. *Colloid Polym Sci* 2000;**278**:369–74.
- Frömer D, Lerche D. An experimental approach to the study of the sedimentation of dispersed particles in a centrifugal field. *Arch Appl Mech* 2002;**72**:85–95.
- Lerche D. Dispersion stability and particle characterization by sedimentation kinetics in a centrifugal field. *J Dispersion Sci Technol* 2002;**23**:699–709.
- Lerche D, Sobisch T. Consolidation of concentrated dispersions of nano- and microparticles determined by analytical centrifugation. *Powder Technol* 2007;**174**:46–9.
- Mirabella FM, Harrick NJ. *Internal reflection spectroscopy: review and supplement*. New York: Harrick Scientific Corporation; 1985.
- Bauer HH, Müller M, Goette J, Merkle HP, Fringeli UP. Interfacial adsorption and aggregation associated changes in secondary – structure of human calcitonin monitored by ATR-FTIR spectroscopy. *Biochemistry* 1994;**33**:12276–82.
- Briscoe BJ, Khan AU, Luckham PF. Optimising the dispersion on an alumina suspension using commercial polyvalent electrolyte dispersant. *J Eur Ceram Soc* 1998;**18**:2141–7.
- Kelso JF, Ferrazzoli TA. Effect of powder surface chemistry on the stability of concentrated aqueous dispersions of alumina. *J Am Ceram Soc* 1989;**72**:625–7.
- Cesarano III J, Aksay IA, Bleier A. Stability of aqueous  $\alpha$ - $\text{Al}_2\text{O}_3$  suspensions with poly(methacrylic acid) polyelectrolyte. *J Am Ceram Soc* 1988;**71**:250–5.
- Vermöhlen K, Lewandowski H, Narres HD, Koglin E. Adsorption of polyacrylic acid on aluminium oxide: DRIFT spectroscopy and ab initio calculations. *Colloids Surf A* 2000;**170**:181–9.

39. Taylor JJ, Sigmund WM. Adsorption of sodium polyacrylate in high solids loading calcium carbonate slurries. *J Colloid Interface Sci* 2010;**341**:298–302.
40. Zaman AA, Tsuchiya R, Moudgil BM. Adsorption of a low-molecular-weight polyacrylic acid on silica, alumina, and kaolin. *J Colloid Interface Sci* 2002;**256**:73–8.
41. Kirwan LJ, Fawell PD, van Bronswijk W. In situ FTIR-ATR examination of poly(acrylic acid) adsorbed onto hematite at low pH. *Langmuir* 2003;**19**:5802–7.
42. Li H, Tripp CP. Interaction of sodium polyacrylate adsorbed on TiO<sub>2</sub> with cationic and anionic surfactants. *Langmuir* 2004;**20**:10526–33.
43. Montavon G, Hennig C, Janvier P, Grambow B. Comparison of complexed species of Eu in alumina-bound and free polyacrylic acid: a spectroscopic study. *J Colloid Interface Sci* 2006;**300**:482–90.
44. Lee DH, Condrate RA, Reed JS. Infrared spectral investigation of polyacrylate adsorption on alumina. *J Mater Sci* 1996;**31**:471–8.
45. Lee DH, Condrate RA. Drift spectral study of polyacrylate (PAA) and polymethyl methacrylate (PMMA) on various ceramics and glasses. *Macromol Symp* 1999;**141**:155–65.
46. Jones F, Farrow JB, van Bronswijk W. An infrared study of a polyacrylate flocculant adsorbed on hematite. *Langmuir* 1998;**14**:6512–7.